Proc. Natl. Acad. Sci. USA
Vol. 86, pp. 3356–3360, May 1989
Medical Sciences

Microvascular sites and characteristics of sickle cell adhesion to vascular endothelium in shear flow conditions: Pathophysiological implications*

DHANANJAYA K. KAUL†, MARY E. FABRY, AND RONALD L. NAGEL

Division of Hematology, Department of Medicine, Albert Einstein College of Medicine and Montefiore Medical Center, Bronx, NY 10461

Communicated by Helen M. Ranney, January 5, 1989

ABSTRACT **To understand the role of sickle cell adherence to the vascular endothelium in the pathophysiology of sickle cell anemia (SS) vasoocclusion, we have carried out a microcirculatory study utilizing the *ex vivo* mesocecum vasculature of the rat. A single bolus of washed oxy-normal (AA) erythrocytes or oxy-SS cells (unseparated or density-defined SS cell classes) was infused. Hemodynamic monitoring and intravital microscopic observations of the microvascular flow revealed higher peripheral resistance for SS erythrocytes and adherence of these cells exclusively to the venular endothelium but rare or no adherence of AA cells. The extent of adhesion was inversely correlated with venular diameters ($r = -0.812$; $P < 0.00001$). The adhesion of SS erythrocytes is density-class dependent: reticulocytes and young discocytes (SS1) > discocytes (SS2) > irreversible sickle cells and unsicklable dense discocytes (SS4). Selective secondary trapping of SS4 (dense cells) is found in postcapillary venules where deformable SS cells are preferentially adhered. We conclude that in the oxygenated condition, vasoocclusion can be induced by two events: (*i*) random precapillary obstruction by a small number of SS4 cells; (*ii*) increased adhesion of SS1 and SS2 cells in the immediate postcapillary venules. A combination of precapillary obstruction, adhesion in postcapillary venules, and secondary trapping of dense cells may induce local hypoxia, increased polymerization of hemoglobin S, and rigidity of SS erythrocytes, thereby extending obstruction to nearby vessels.**

The polymerization of hemoglobin S, which results in increased rigidity of erythrocytes, is central but may not be the exclusive causal factor responsible for the onset of a sickle cell (SS) induced vasoocclusive episode. The lack of correlation between the percent dense cells and incidence of painful crisis (1) suggests that factors other than intracellular polymerization might be involved (2). Increased adhesion of sickle cells could be an additional factor and was first demonstrated by Hebbel *et al.* (3, 4) and later confirmed in both static and flowing systems with cultured endothelial cells obtained from human and other mammalian sources by several investigators (5–10). Nevertheless, whether the increased adherence of sickle cells to the endothelium may potentially contribute to vasoocclusion has not yet been evaluated in a living microvascular network.

The erythrocytes in sickle cell anemia patients are heterogeneous in density, morphological characteristics, and function (11–15), but the relative contribution of individual sickle cell classes to adhesion and obstructive events has not been demonstrated in a perfused microvasculature.

Since sickle cell vasoocclusion in a microcirculatory event, contributions from microvascular factors such as the vessel wall features, topography, and prevailing wall shear rates will be critical to the microvascular obstruction (16) and to secondary trapping or adhesion of individual sickle cell classes. No direct microcirculatory study has been performed to show specific sites of sickle cell adhesion and their topographical characteristics.

In the present study, we have used an *ex vivo* assay of erythrocyte adherence that approximates the shear flow conditions encountered by erythrocytes *in vivo*. The following issues were addressed: (*i*) Does sickle cell–endothelial cell interaction take place in a living microvascular network during flow conditions? (*ii*) Are there preferential sites of adhesion in the branching orders of the microvasculature? (*iii*) What is the relative contribution of sickle cell density classes to adhesion and obstructive events when density-defined mixtures are used?

MATERIALS AND METHODS

Preparation of Cells. Fresh heparinized blood samples were obtained by venipuncture of normal adults ($n = 6$) and from stable sickle cell patients ($n = 7$) who had not had painful crisis or blood transfusions in the preceding 4 months. The samples were centrifuged (2000 rpm) and the plasma and buffy coat were removed. Unseparated AA and SS erythrocytes were then washed three times in 0.9% NaCl, once in bicarbonate Ringer's solution (118 mM NaCl/5.0 mM KCl/2.5 mM $CaCl_2$/0.64 mM $MgCl_2$/27.0 mM $NaHCO_3$/0.5% bovine serum albumin) and finally resuspended in oxygenated bicarbonate Ringer's equilibrated with 94.4% O_2/5.6% CO_2, pH 7.4.

Blood was separated into density-defined fractions with Percoll (colloidal silica coated with polyvinylpyrrolidone; Pharmacia), and Stractan (arabinogalactan polysaccharide; St. Regis Paper, West Nyack, NY) (prepared as described by Corash *et al.* in ref. 17) density gradients were formed as described (11). The density gradient procedure is shown to have no effect on the morphology and mean corpuscular hemoglobin concentration (MCHC) of different classes of sickle cells (11, 12). MCHC was measured by using handspun hematocrit (Hct) and Drabkin's reagent. Reticulocytes were stained with methylene blue and irreversibly sickled cell (ISC) counts were made in the neutral formalin.

Sickle cell density fractions were washed three times in 0.9% NaCl to remove the gradient mixture. For fluorescent-labeling of erythrocytes, fluorescein isothiocyanate (FITC) was dissolved at pH 9.0 in phosphate-buffered saline (PBS) (137 mM NaCl/2.7 mM KCl/8.1 mM Na_2HPO_4/1.5 mM KH_2PO_4, pH adjusted with 0.15 M NaOH; osmolarity, 285 mosM) at a concentration of 2 mg/ml. Next, 5 ml of this

Abbreviations: FITC, fluorescein isothiocyanate; Hct, hematocrit; ISC, irreversibly sickled cells; MCHC, mean corpuscular hemoglobin concentration; PRU, peripheral resistance unit; Tpf, pressure-flow recovery time.

*This work was presented at the Annual Meeting of the American Federation of Clinical Research, April 29–May 2, 1988 (35).

†To whom reprint requests should be addressed.

The publication costs of this article were defrayed in part by page charge payment. This article must therefore be hereby marked "*advertisement*" in accordance with 18 U.S.C. §1734 solely to indicate this fact.

solution was added to 0.5 ml of packed cells from a given fraction. The mixture was incubated for 1 hr at 24°C, using gentle agitation every 10 min to achieve uniform labeling of erythrocytes (18). The labeled erythrocytes were washed four times with PBS (pH 7.4), once in oxygenated bicarbonate Ringer's, and finally were resuspended in Ringer's. Densitometric analysis of gradient images of unseparated SS or AA erythrocytes labeled with FITC (1–4 mg/ml) showed no significant changes in the overall density distribution of these cells as compared with their unlabeled counterparts. The unlabeled sickle cell fractions were washed three times in PBS and similarly resuspended in the oxygenated bicarbonate Ringer's. In each case, Hct was adjusted to 30%.

Artificially Perfused Mesocecum Microvasculature. Perfusion studies were performed in the isolated, acutely denervated, and artificially perfused rat mesocecum microvasculature ($n = 20$) according to the method of Baez *et al.* (19) as modified by Kaul *et al.* (20) for the infusion of erythrocytes. Details of the procedure have been described elsewhere (12).

Hemodynamic Monitoring. Arterial perfusion pressure (Pa) was rendered pulsatile with a peristaltic pump. Control Pa and the venous outflow pressure (Fv) were kept constant at 70 and 3.8 mmHg, respectively. Venous outflow (Fv) was monitored with a photoelectric dropcounter and expressed as ml/min. During constant perfusion with Ringer's, a bolus (0.2 ml) of a given erythrocyte sample (Hct 30) was gently delivered via an injection port proximal to arterial cannulation. Peripheral resistance units (PRU) were determined and expressed as PRU = $\Delta P/Q$ = mmHg·ml^{-1}·min^{-1}·g^{-1}, where ΔP is the arteriovenous pressure difference and Q is the rate of venous outflow (Fv) per g of tissue (21). Pressure flow recovery time (Tpf) was determined (20) as time (seconds) required for Pa and Fv to return to their baseline levels after bolus delivery.

Microcirculatory Observations and Quantitation of Erythryocyte Adherence. Direct microscopic observations and video monitoring of the microcirculatory events were carried out using an Olympus microscope (model BH-2) equipped with both bright-field transillumination and fluorescence Ploem epiillumination. The video recording system consisted of a television camera (Cohu, 5000 Series), an Ikegami monitor, and a Panasonic video recorder (model NV9300A).

After the passage of the bolus, the microvasculature was examined for adherent sickle cells and vascular segments were scanned and videotaped according to topological order. The number of adherent sickle cells per 100 μm^2, using this topological scheme, was calculated from the counts of individual adherent cells and the surface area (μm^2) of the inner wall of the vessel segment. The surface area is expressed as: surface area (μm^2) = $(2\pi r)(l)$, where r is the radius of the vessel lumen and l is the vessel length. The number of adherent cells per 100 μm^2 was calculated as follows:

$$\text{number of adherent cells/100 } \mu m^2 = \frac{\text{number of adherent cells}}{\text{surface area } (\mu m^2)} \times 100.$$

The relative adherence of a given sickle class in a mixture of two density-defined classes (one of them labeled with FITC) was determined from the numbers of FITC-labeled versus unlabeled cells in each venular segment using epifluorescence and transillumination. FITC labeling did not affect hemodynamic and microcirculatory behavior of unseparated erythrocytes, as determined for pairs of unlabeled and labeled AA or SS erythrocytes in three preliminary experiments. Also, there was no evidence of any fluorescent cross-labeling of any vessel component (see Fig. 3) after the bolus infusion of mixed sickle cell classes.

Statistical analysis of the data was carried out using the program STATGRAPHICS 2.4 and an IBM-AT computer.

RESULTS

Table 1 gives data on hemodynamic parameters (PRU and Tpf) for each category of experiments. Infusion of SS erythrocytes invariably resulted in higher PRU and delayed or partial recovery of pressure and flow as compared to control AA cells. In each case, the passage of AA erythrocytes was uninterrupted and followed by rapid recovery of pressure and flow.

Directed microscopic observations and simultaneous videotaping revealed rare or no adhesion of normal erythrocytes to the vascular endothelium. This behavior of AA cells is in conformity with our earlier observations (22). In contrast, the infusion of unseparated SS erythrocytes ($n = 4$) invariably resulted in adhesion of a significant number of these cells exclusively to the venular endothelium. After the passage of bolus, adherent sickle cells could be observed in the venules of various diameters during perfusion with Ringer's solution. In shear flow conditions, individual SS erythrocytes were found tethered to the endothelium and could be seen aligned in the direction of flow (Fig. 1*A*). Counts of adherent SS cells in the affected venules showed that the extent of adhesion was inversely correlated with venular diameters (using the equation $y = ax^b$; $y = 1.0689x^{-1.1206}$, $r = -0.812$, $r^2 = 0.659$, $P < 0.00001$), as the number of adherent cells per 100 μm^2 was highest in the immediate postcapillary venules (Fig. 2). In some instances, these narrow venules (diameter, 7–10 μm) displayed complete lumen obstruction (Fig. 1*B*), which precluded counting.

Next, we evaluated relative adherence of SS cell density classes present in unseparated SS blood. Selective fluorescent labeling with FITC was used to identify a given SS density class in a mixture. FITC-labeling of erythrocytes (SS or AA) did not alter their density profiles or their hemody-

Table 1. Perfusion experiments with normal (AA) and sickle (SS) erythrocytes

Cells	n	PRU, mmHg·ml^{-1}·min^{-1}·g^{-1}		PRU, % increase	Tpf, sec
		Ringer's	Cells		
AA	15	6.1 ± 1.0	7.7 ± 1.7	26.4 ± 15.1	61.8 ± 26.0
SS, unseparated	4	6.3 ± 1.9	9.6 ± 4.1	48.3 ± 20.3*	Delayed to partial recovery
SS2 + SS4 (3:1)	7	6.9 ± 1.4	14.6 ± 4.1	110.4 ± 30.1†	Partial recovery
SS2 + SS4 (1:1)	3	7.4 ± 0.9	16.0 ± 4.9	136.7 ± 82.1‡	Partial recovery
SS1 + SS2 (1:1)	3	5.4 ± 0.7	9.5 ± 1.6	77.9 ± 28.7§	97.8 ± 19.7¶

Values are means ± SD. Density-defined sickle cell populations: SS1 has low MCHC (31–33 g/dl) and consists of reticulocytes and young discocytes; SS2 cells have normal MCHC (34–36 g/dl) and normal biconcave shape; SS4 cells have increased MCHC (41–46 g/dl) and abnormal shapes (ISC and unsicklable dense granular discocytes). Ratios of SS fractions in mixtures are indicated in parentheses. Mesocecum preparations obtained from different animals show some variations in the venous outflow due to anatomical and vascular topographical variations. These differences are reflected in PRU for Ringer's. *$P < 0.0277$; †$P < 0.000000024$; ‡$P < 0.00005$; §$P < 0.0003$; ¶$P < 0.016$. In these experiments comparisons were made with normal erythrocytes.

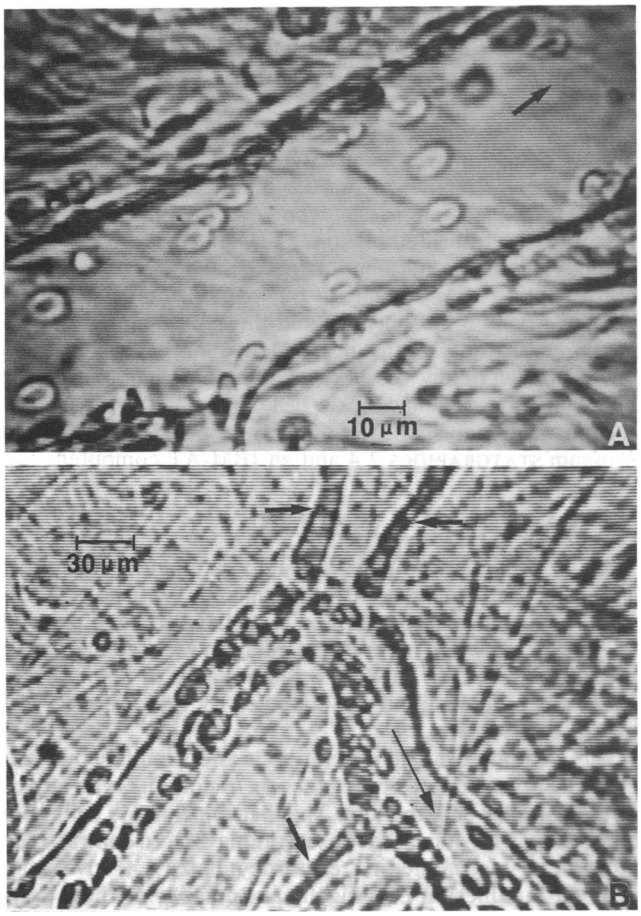

FIG. 1. Adhesion of sickle erythrocytes in venules. (*A*) Adherent sickle cells of discocytic morphology are seen tethered to the endothelial wall of a venule and are aligned in the direction of the flow (arrow). (*B*) Increased adhesion of sickle cells at venular bending and at junctions of smaller diameter postcapillary venules. In this instance, the postcapillary vessels (small arrows) are totally blocked. Large arrow indicates flow direction.

namic and microcirculatory behavior. In a series of experiments (n = 7), relative adhesivity of fraction SS2 (mainly discocytes) and fraction SS4 (dense unsicklable granular dense discocytes and 33–55% ISC) was compared in each vasculature under the same flow conditions. Either fraction (SS2 or SS4) was labeled with FITC and the two fractions were then mixed just prior to the infusion (3 parts of SS2 and 1 part of SS4, both Hct 30). Infusion of the SS2 and SS4 cell mixture resulted in incomplete recovery of pressure and flow (Table 1), which is indicative of some microvascular blockage. Adhesion was again confined to the venules and the total number of adhered erythrocytes from both density classes per 100 μm^2 showed the same pattern of inverse correlation with venular diameters as was noted for unseparated SS cells

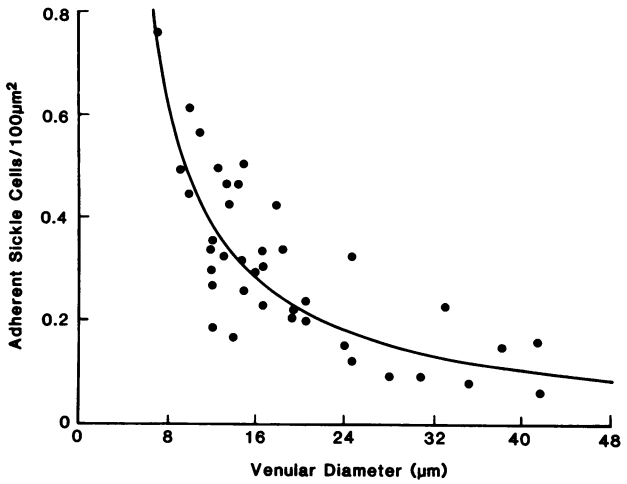

FIG. 2. Relationship between venular diameter and sickle erythrocyte adhesion (unseparated cells) in the venules of mesocecum microvasculature. The regression fits the equation $y = 1.0689x^{-1.1206}$, $r = -0.812$, $r^2 = 0.659$, $P < 0.00001$.

($y = 1.8613x^{-1.4981}$, $r = -0.789$, $r^2 = 0.623$, $P < 0.00001$). The mean of all adherent SS2 and SS4 cells per 100 μm^2 was not significantly different from the mean values for unseparated samples (Table 2), which is due to the dominance of SS2 cells in each case. Differential counts of adherent SS2 and SS4 cells using epifluorescence and transillumination revealed that irrespective of the fraction labeled, SS2 cells showed preponderance over SS4 cells. Of the total number of adherent cells in the venular segments, adherent SS2 cells outnumbered SS4 cells by a ratio of almost 12:1 (Table 2). In a separate group of three experiments in which SS2 and SS4 were mixed in a 1:1 ratio (both Hct 30) and either fraction was labeled with FITC, the infusion resulted in partial recovery of pressure and flow (Table 1), indicating microvascular blockage. The adhesion again showed strong inverse correlation with the venular diameter ($y = 2.29x^{-1.6638}$, $r = -0.911$, $r^2 = 0.83$, $P < 0.00001$). In the areas of adhesion, SS2 cells had clear-cut preponderance over SS4 cells by a ratio of almost 3:1 (Table 2). The absence of significant differences in the mean of all adherent cells (SS2 and SS4) in 1:1 mixtures, as compared to that of unseparated samples or the 3:1 mixtures (Table 2), can be related to the higher ratio of dense SS4 cells. In other words, the impaired flow behavior (Table 1) of 1:1 mixtures would cause increased interaction of erythrocytes with the endothelium despite the lower ratio of SS2 cells in these mixtures. The presence of unusually high concentrations of SS4 cells in totally obstructed postcapillary venules of various diameters (Fig. 3 *A* and *B*) is of particular interest. Such selective trapping of SS4 cells was repeatedly observed in these experiments. In contrast to SS2 cells, no correlation between adherent SS4 cells and venular diameters was noted. Occasionally, venular capillaries (diameter, 4.5–6.0 μm) were seen obstructed with a single file of cells containing a

Table 2. Sickle cell adherence to the endothelium of venules and relative adherence of density-defined fractions

Infused cells (SS)	No. of venules	Mean venular diameter, μm	Mean venular length, μm	All adherent cells per 100 μm^2	Relative adherence of fractions, %		
					SS1	SS2	SS4
Unseparated cells	39	19.0 ± 8.9	132.2 ± 83.3	0.30 ± 0.16	—	—	—
SS2 + SS4 (3:1)	39	18.1 ± 7.1	98.7 ± 27.9	0.33 ± 0.21	—	92.2 ± 8.9	7.8 ± 8.9*
SS2 + SS4 (1:1)	34	22.8 ± 15.2	162.6 ± 119.0	0.35 ± 0.26	—	74.5 ± 17.2	26.2 ± 16.7*
SS1 + SS2 (1:1)	44	21.3 ± 10.3	146.4 ± 82.4	0.36 ± 0.27	64.2 ± 10.9	35.7 ± 11.0†	—

Values are means ± SD. SS fractions were mixed in ratios indicated in parentheses. In a given mixture, either fraction was selectively labeled with FITC.

*Differentiation in the mean relative adherence (%) of fractions SS2 and SS4 in both experiments was significant at $P < 0.00001$.

†Difference in the mean relative adherence (%) of SS1 and SS2 was significant at $P < 0.00001$.

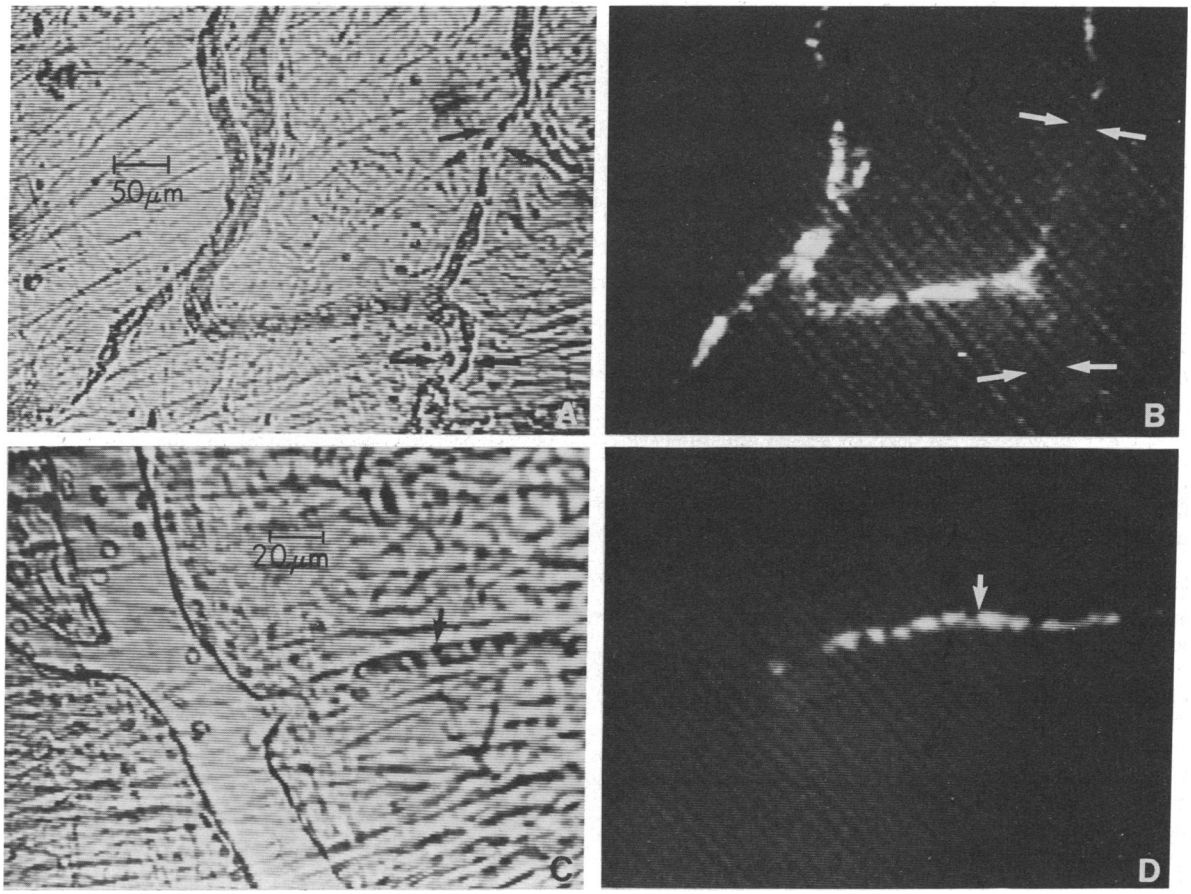

FIG. 3. Selective trapping of dense cells (fraction SS4) in postcapillary venules and obstruction in a venular capillary after infusion of a mixture of fraction SS2 (discocytes) and FITC-labeled fraction SS4 (ISC and dense unsicklable discocytes) mixed in a ratio of 3:1. (*A*) Areas of venular obstruction. Arrows indicate unobstructed areas showing only adherent cells. (*B*) The same area seen under epifluorescence illumination showing high concentration of FITC-labeled dense fraction SS4 cells trapped in the obstructed venules of various diameters and their absence in areas with adhesion but without lumen obstruction (arrows). (*C*) A venular capillary is seen obstructed with a single file of cells and joins a large diameter venule, which shows individual adhered discocytic cells. (*D*) The same area seen under epifluorescence illumination. Fluorescent dense cells obstruct the venular capillary but are absent in the venule.

mixture of SS2 and SS4 cells (Fig. 3 *C* and *D*). In such cases, adhesion cannot be established or denied. In addition, trapping of SS4 cells, especially ISC, occurred randomly at arteriolar–capillary bifurcations and venular junctions.

A similar evaluation of fraction SS1 (reticulocytes and young discocytes) and SS2 cells was carried out with selective fluorescent labeling of either fraction. Infusion of SS1 and SS2 cells, mixed in a 1:1 ratio (both Hct 30), resulted in higher PRU and delayed Tpf when compared to normal cells (Table 1), suggesting increased resistance during capillary transit. Once again, the adhesion was confined to the venules and the number of all adherent cells per 100 μm^2 showed strong inverse correlation with venular diameters ($y = 1.5594x^{-1.2737}$, $r = -0.856$, $r^2 = 0.733$, $P < 0.00001$). In the areas of adhesion, SS1 cells outnumbered SS2 cells by a ratio of almost 2:1 (Table 2). In the three experiments in which the percentages of reticulocytes in the infused mixtures were 15.8, 29.8, and 57.9, the corresponding mean values for all adherent cells per 100 μm^2 in the venules were 0.25 ± 0.13, 0.41 ± 0.31, and 0.44 ± 0.31, respectively (means ± SD). The difference between mean adherent cells for samples containing 15.8% and 57.9% reticulocytes was significant ($P < 0.038$). Since the mean value for all unseparated samples (reticulocyte counts, 5–16%) was intermediate between that obtained for the very low reticulocyte artificial mixture (% reticulocytes = 15.8) and the very high reticulocyte mixture (% reticulocytes = 57.9), the mean of the unseparated samples was not statistically different from the two extreme values.

Topographical analysis revealed that adhesion of SS erythrocytes occurred more frequently at vessel bendings and near vessel junctions (Fig. 1*B*), although adhesion was also recorded in straight venular segments without junctions. Only few adhered cells were seen detaching during flow, although in many instances transitory adhesion of SS cells occurred as the cells rolled briefly along the venular wall before rejoining the flow. Rolling cells were not included in the count of adhered cells.

DISCUSSION

The present study, utilizing perfusion conditions approximating *in vivo* flow, reveals that sickle erythrocytes adhere exclusively to the endothelium of venules in inverse correlation with the vessel diameter. Our experimental approach using the perfused mesocecum vasculature, which has the characteristics of *in vivo* endothelial architecture, vascular topographical features, and microvascular shear flow encountered *in vivo* by erythrocytes, differs markedly from earlier studies in which cultured endothelial cells in static or flowing systems were used to demonstrate increased adhesion of SS erythrocytes (3–10).

The maximum concentration of adherent cells per 100 μm^2 is observed in the immediate postcapillary venules (diameter, 7–10 μm) where the number of adhered cells may reach as

high as 1.0 per 100 μm^2. When the concentration of adhered cells increases above this level, the vessels may be blocked. This correlation appears to be determined by the arteriovenous erythrocyte velocity and wall shear rate gradients. In the microcirculation, both erythrocyte velocity and wall shear rates are highest in the arterioles but drop steeply as erythrocytes traverse from capillaries to the immediate postcapillary vessels before rising again in larger venules (23, 24). Thus, the immediate postcapillary vessels provide the maximum opportunity for circulating erythrocytes to interact with the endothelium. In the postcapillary venules, the wall shear rates can be as low as 100 sec^{-1}, while on the arteriolar side, these can exceed 1000 sec^{-1} (13, 23, 24), which probably precludes erythrocyte adhesion. Decreased sickle cell adherence to cultured endothelium is also noted with increased wall shear rates in larger gap-width flow systems (>100 μm) (8, 9). The topographical features of adhesion sites include vessel bendings and junctions and support the observations of Burn *et al.* (7).

We find that density-defined sickle cell classes show significant differences in their adhesivity. During shear flow conditions, the dense SS4 fraction (ISC and unsicklable dense granular discocytes) was found to be least adherent while the least dense cells' cellular component (fraction SS1: reticulocytes and young discocytes) showed maximum propensity for adhesion. The discocyte fraction SS2, the predominant cellular component of SS blood, showed intermediate adhesivity. These differences in adhesivity were recorded when these cell classes were infused in density-defined mixtures under the same shear flow conditions, rather than for each fraction individually. These results are in concordance with the *in vitro* studies of Barabino *et al.* (9, 25) and Mohandas and Evans (26), who studied individual fractions but not mixtures. The most dense cells (SS4) are hemodynamically least competent (12) because of shape irregularities and high MCHC and are also the least adherent. As pointed out by Barabino *et al.* (25), the abnormal shape of ISCs and dense cells is likely to minimize the areas of interaction and prevent prolonged contact with the surface of the endothelial cells. Furthermore, interactions between hemodynamically different erythrocyte density classes may play a role.

Although the experiments reported here were conducted with washed erythrocytes, they cannot be interpreted as evidence that "plasma" factors are not involved. Indeed, an *ex vivo* preparation is capable of discharging into the circulation endothelium-derived molecules that can be involved in the adhesion process (27). Wick *et al.* (28) have suggested that endothelium-derived large multimers of von Willebrand factor might play a role and these could be present in our preparation. We find that significant adhesion of normal erythrocytes (27) and a manyfold increase in the adhesion of sickle cells (29) occur when the *ex vivo* preparation is perfused with desmopressin, an analogue of vasopressin that causes release of stored von Willebrand factor. These observations indicate that adhesion probably involves factors directly associated with the endothelium and erythrocytes.

Another interesting point is the role of dense cells in the obstructive events. Although fraction SS4 is found to be the least adherent of all, it invariably contributes to the observed obstruction of postcapillary venules. It appears that the increased adhesion of more deformable density classes (SS1, SS2) in the immediate postcapillary venules may result in a sieve-like formation conducive to selective secondary trapping of less deformable dense SS4 cells. In the areas of total obstruction, this pattern of dense cell trapping was repeatedly observed. The present intravital observations provide direct support to our earlier studies demonstrating the presence of disproportionate high concentrations of dense cells in samples eluted from the obstructed areas (15) and explain the disappearance of dense cells from the peripheral blood during sickle cell painful crisis (30). Thus, the ISC-rich SS4 fraction may contribute to obstruction either by blocking the narrow vessel lumen already lined with adherent less dense sickle cells or occasionally by direct capillary occlusion (Fig. 3 *C* and *D*) or by initiating obstruction at vessel junctions especially at the arteriolar–capillary bifurcation points. The latter obstructive event appears to be random and its occurrence cannot be predicted in a given microvascular bed, as also noted in previous studies (31–34). Such secondary trapping may induce local hypoxia and result in increased polymerization of hemoglobin, thereby propagating the obstruction to nearby vessels.

This work was supported by grants from the American Heart Association (New York Affiliate) and the New York Community Trust and by Project Grant HL-21016 from the National Heart, Lung, and Blood Institute.

1. Billett, H. H., Kim, K., Fabry, M. E. & Nagel, R. L. (1986) *Blood* **68**, 301–303.
2. Nagel, R. L., Fabry, M. E., Billett, H. H. & Kaul, D. K. (1987) *Prog. Clin. Biol. Res.* **240**, 361–380.
3. Hebbel, R. P., Yamada, O., Moldow, D. F., Jacob, H. S., White, J. G. & Eaton, J. W. (1980) *J. Clin. Invest.* **65**, 154–160.
4. Hebbel, R. P., Boogaerts, M. A., Eaton, J. W. & Steinberg, M. H. (1980) *N. Engl. J. Med.* **302**, 992–995.
5. Hoover, R., Rubin, R., Wise, G. & Warren, R. (1979) *Blood* **54**, 872–876.
6. Mohandas, N. & Evans, E. (1985) *J. Clin. Invest.* **76**, 1605–1612.
7. Burns, E. R., Wilkinson, W. H. & Nagel, R. L. (1985) *J. Lab. Clin. Med.* **104**, 673–678.
8. Smith, B. D. & LaCelle, P. L. (1986) *Blood* **68**, 1050–1054.
9. Barabino, G. A., McIntire, L. V., Eskin, S. G., Sears, D. A. & Udden, M. (1987) *Blood* **70**, 152–157.
10. Grabowski, E. F. (1987) *Prog. Clin. Biol. Res.* **240**, 167–179.
11. Fabry, M. E. & Nagel, R. L. (1982) *Blood Cells* **8**, 9–15.
12. Kaul, D. K., Fabry, M. E., Windisch, P., Baez, S. & Nagel, R. L. (1983) *J. Clin. Invest.* **72**, 22–31.
13. Kaul, D. K., Nagel, R. L. & Baez, S. (1983) *Microvasc. Res.* **26**, 170–181.
14. Lipowsky, H. L., Sheikh, N. U. & Katz, D. M. (1987) *J. Clin. Invest.* **80**, 117–127.
15. Kaul, D. K., Fabry, M. E. & Nagel, R. L. (1986) *Blood* **68**, 1162–1166.
16. Kaul, D. K. (1988) in *Genetically Abnormal Red Cells*, ed. Nagel, R. L. (CRC, Boca Raton, FL), Vol. 2, pp. 161–176.
17. Corash, L. M., Piomelli, S., Chen, H. C., Seaman, C. & Gross, E. (1974) *J. Lab. Clin. Med.* **84**, 147–151.
18. Matuhasi, T., Usui, M. & Nariuchi, H. (1971) *Ann. N.Y. Acad. Sci.* **177**, 467–480.
19. Baez, S., Lamport, H. & Baez, A. (1960) in *Flow Properties of Blood and Other Biological Systems*, eds. Copley, A. L. & Stainsby, G. (Pergamon, London), pp. 122–136.
20. Kaul, D. K., Baez, S. & Nagel, R. L. (1981) *Clin. Hemorheol.* **1**, 73–86.
21. Green, H. D., Rapela, C. E. & Conard, M. D. (1963) in *Handbook of Physiology: Circulation*, eds. Hamilton, W. F. & Stainsby, G. (Am. Physiol. Soc., Bethesda, MD), Vol. 2, pp. 935–960.
22. Raventos-Suarez, C., Kaul, D. K., Macaluso, F. & Nagel, R. L. (1985) *Proc. Natl. Acad. Sci. USA* **82**, 3829–3833.
23. Lipowsky, H. H., Kovalcheck, S. & Zweifach, B. W. (1978) *Circ. Res.* **43**, 738–749.
24. Zweifach, B. W. & Lipowsky, H. H. (1984) in *Handbook of Physiology: Cardiovascular System*, eds. Renkin, E. M. & Geiger S. R. (Am. Physiol. Soc., Bethesda, MD), Vol. 4, pp. 251–307.
25. Barabino, G. A., McIntire, L. V., Eskin, S. G., Sears, D. A. & Udden, M. (1987) *Prog. Clin. Biol. Res.* **240**, 113–127.
26. Mohandas, N. & Evans, E. (1987) *Prog. Clin. Biol. Res.* **240**, 181–190.
27. Tsai, H. M., Sussman, I. I., Nagel, R. L. & Kaul, D. K. (1988) *Blood* **36**, 409A (abstr.).
28. Wick, T. M., Moake, J. L., Udden, M. M., Eskin, S. G., Sears, D. A. & McIntire, L. V. (1987) *J. Clin. Invest.* **80**, 905–910.
29. Kaul, D. K., Sussman, I. I., Tsai, H. M. & Nagel, R. L. (1989) *Clin. Res.* (abstr.), in press.
30. Fabry, M. E., Benjamin, L., Lawrence, C. & Nagel, R. L. (1984) *Blood* **64**, 559–563.
31. Klug, P. P. & Lessin, L. S. (1977) *Blood Cells* **3**, 263–272.
32. LaCelle, P. L. (1977) *Blood Cells* **3**, 273–282.
33. Lipowsky, H. H., Usami, S. & Chien, S. (1982) *Blood Cells* **8**, 113.
34. Baez, S., Kaul, D. K. & Nagel, R. L. (1982) *Blood Cells* **8**, 127–137.
35. Kaul, D. K., Fabry, M. E. & Nagel, R. L. (1988) *Clin. Res.* **36**, 412 (abstr.).